SLIMEr: probing flexibility of lipid metabolism in yeast with an improved constraint-based modeling framework

Benjamín J. Sánchez[1,2], Feiran Li[1,2], Eduard J. Kerkhoven[1,2] and Jens Nielsen[1,2,3(*)]

[1] Department of Biology and Biological Engineering, Chalmers University of Technology, Gothenburg, Sweden

[2] Novo Nordisk Foundation Center for Biosustainability, Chalmers University of Technology, Gothenburg, Sweden

[3] Novo Nordisk Foundation Center for Biosustainability, Technical University of Denmark, Lyngby, Denmark

(*) Corresponding author.

Correspondence: nielsenj@chalmers.se

Summary

A recurrent problem in metabolic modeling is to correctly represent lipid species incorporated into biomass, due to the numerous of possible combinations of individual lipid species. In this study, we developed SLIMEr, a formalism for correctly modeling lipid metabolism in genome-scale metabolic models. We achieve this by enhancing a model with mathematical constructs where we Split Lipids Into Measurable Entities (SLIME reactions), in addition to constraints on both the lipid classes and the acyl chain distribution. By implementing this method for the consensus genome-scale model of *Saccharomyces cerevisiae*, we can predict accurate amounts of lipid species, analyze the flexibility of the resulting distribution, and compute the energy costs of moving from one metabolic state to another. The approach shows potential for better understanding lipid metabolism in yeast under different conditions. SLIMEr is freely available at https://github.com/SysBioChalmers/SLIMEr.

Keywords: Genome-scale metabolic modeling, *Saccharomyces cerevisiae*, lipidomics, flux balance analysis.

1. Introduction

Genome scale metabolic models (GEMs) are widely used to model and compute functional states of cellular metabolism (Nielsen, 2017). A crucial step for achieving these simulations is to define a biomass pseudo-reaction (Feist & Palsson, 2010; Dikicioglu *et al*, 2015), which accounts for every single constituent comprising the cellular biomass (proteins, carbohydrates, lipids, etc.). In this step it is challenging to account for lipid requirements, as there are copious different individual lipid species: over 20 different classes of lipids can be produced in a cell, and each specific lipid belonging to any of those classes can contain various combinations of acyl chain groups, each of them with varying length and number of saturations (Ejsing *et al*, 2009). This can yield over 1000 specific lipid species that the cell can potentially produce. Unsurprisingly, lipid metabolism therefore tends to be the most complicated part of any GEM.

In addition, a necessary requirement for formulating the biomass pseudo-reaction is to have abundance measurements [mmol/gDW] of every single constituent; however, this is seldom available for individual lipid species; what is more common is to instead measure separately (i) a profile of all different lipid classes, with high-performance liquid chromatography (Khoomrung *et al*, 2013), and (ii) a distribution of all different acyl chains, with fatty acid methyl ester (FAME) analysis (Abdulkadir & Tsuchiya, 2008). GEMs need to therefore handle these types of data.

The most common approach to represent lipid metabolism in GEMs is to enforce a specific distribution of each individual lipid species, either by using experimental data (Mardinoglu *et al*, 2014; Lachance *et al*, 2018) or by assuming that lipid classes have all the same acyl-chain distribution from FAME analysis (Nookaew *et al*, 2008; Kerkhoven *et al*, 2016). In both cases however, the model is fixed to follow the predefined lipid distribution, even if simulations are run under experimental conditions that might affect lipid metabolism. A second approach is to allow any specific lipid to form a corresponding generic lipid class (e.g., “phosphocholine”) and to only constrain those classes with experimental abundances from lipid profiling (Heavner *et al*, 2012; Brunk *et al*, 2018). The problem with this approach is that experimental abundances from FAME analysis are neglected, and simulations always end up choosing lipid species that cost the least energy, which might not reflect reality, e.g. if there is regulation in place to ensure production of

longer chain species. Hence there is need for an approach that can incorporate both lipid profiling and FAME, but at the same time allow network flexibility.

In this work, we introduce SLIMEr, an enhanced constrained-based modeling framework for lipid metabolism. The approach is based on the introduction of so called SLIME reactions, which split lipids into their basic components; and lipid pseudo-reactions, that impose constraints on both the lipid classes and the acyl chain distributions. By following this approach, we achieve flux simulations that respect the acyl chain experimental distribution, and at the same time avoid over-constraining the model to only simulate one lipid distribution. We implemented this approach for the consensus GEM of *Saccharomyces cerevisiae* (budding yeast), a model that has undergone iterative improvements (Herrgård *et al*, 2008; Dobson *et al*, 2010; Heavner *et al*, 2012, 2013; Aung *et al*, 2013) and is currently being hosted at https://github.com/SysBioChalmers/yeast-GEM. We show that the enhanced model can better represent lipid requirements for metabolism, has a high degree of flexibility, and can simulate how lipid costs change at varying experimental conditions.

2. Methods

2.1. FBA and the challenge of representing lipid composition

Flux balance analysis (FBA) (Orth *et al*, 2010) is based on the following assumptions on metabolism: (i) a cell has a metabolic goal, which we can represent through a mathematical objective function, (ii) under short timescales there is no accumulation of intracellular metabolites, and (iii) metabolic fluxes are bounded to physical constraints, such as thermodynamics and kinetics. Those 3 assumptions define a basic FBA problem as followed:

$$\begin{aligned} &\mathrm{Min}(c^{T}v) \\ &S \cdot v = 0 \qquad [\mathrm{Eq.}\,1] \\ &LB \leq v \leq UB \end{aligned}$$

where S is the stoichiometric matrix, which contains the stoichiometric coefficients for all reactions and metabolites, v is the vector of metabolic fluxes [mmol/gDWh], c is the objective function vector, and LB and UB are the corresponding lower and upper bounds for each of the

fluxes (some of them based on experimental values). As we usually wish to simulate growth, a biomass pseudo-reaction is typically added to the stoichiometric matrix as follows:

$$\text{protein} + \text{carbohydrate} + \text{lipid} + \text{RNA} + \text{DNA} + \cdots \rightarrow \text{Biomass} \qquad [\text{Eq.}\,2]$$

where protein, carbohydrate, lipid, etc., are pseudo-metabolites that are produced from a combination of metabolic components. For example, protein is produced from a protein pseudo-reaction:

$$s_1\ \text{ala} + s_2\ \text{cys} + s_3\ \text{asp} + \cdots \rightarrow \text{protein} \qquad [\text{Eq.}\,3]$$

where s_i are the measured abundances [mmol/gDW] of the corresponding amino acids in yeast. In this study we focus on the lipid pseudo-reaction, which becomes more challenging to formulate, because there are so many different individual species. One option is to define an equivalent reaction to Eq.3 with every single lipid species (Mardinoglu *et al*, 2014); however, as these measurements are not available for most organisms, the lipid pseudo-reaction is usually represented as the following instead:

$$s_1\ \text{PI} + s_2\ \text{PC} + s_3\ \text{TAG} + s_4\ \text{ERG} \ldots \rightarrow \text{lipid} \qquad [\text{Eq.}\,4]$$

where PI (phosphoinositol), PC (phosphocholine), TAG (triglyceride), ergosterol (ERG), etc. represent each of the lipid classes that exist in the model. Most of them represent not one but a plurality of different molecules, each with different combinations of acyl chain lengths and saturations. Therefore, they are also pseudo-metabolites that need to be produced in turn by additional pseudo-reactions. These pseudo-reactions can be constructed either in a restrictive or permissive approach (Figure 1). The restrictive approach is to enforce the experimental FAME distribution to every single specific lipid species. This can be achieved by creating a generic acyl chain component (Nookaew *et al*, 2008):

$$s_1\text{Acyl} - \text{CoA}(16{:}0) + s_2\text{Acyl} - \text{CoA}(16{:}1) + \cdots \rightarrow \text{AcylCoA} \qquad [\text{Eq.}\,5]$$

where the s_i coefficients are inferred from FAME data. This generic Acyl – CoA is then used to form each generic lipid species, forcing then every class to have the same acyl chain distribution. The problem of this approach is that the model will be fixed to always follow the same lipid distribution. On the other hand, the permissive approach for building the pseudo-reactions is to allow any of the specific lipids to form the generic lipid class (Heavner *et al*, 2012). For instance, the following set of pseudo-reactions are defined for PI:

$$\begin{aligned} &\mathrm{PI}\ (16{:}0 - 16{:}1) \rightarrow s_1\mathrm{PI} \\ &\mathrm{PI}\ (16{:}1 - 16{:}1) \rightarrow s_2\mathrm{PI} \qquad [\mathrm{Eq.}\,6] \\ &\mathrm{PI}\ (16{:}1 - 18{:}1) \rightarrow s_3\mathrm{PI} \\ &\qquad\vdots \end{aligned}$$

where s_i can be set to 1 or adapted to represent the cost of producing each specific lipid. The problem of this approach is that it disregards the acyl chain distribution, even if FAME data is available. Therefore, once simulations are computed, the model will always end up preferring the "cheapest" species to produce in terms of carbon and energy, usually corresponding to species with the shortest acyl chains, unless the s_i coefficients are arbitrarily tuned to favor longer chains. Finally, even though for some specific species such as ergosterol the measured abundance [mg/gDW] can be directly transformed to the stoichiometric coefficient in Eq.4 [mmol/gDW], for the case of most lipids the measured abundance cannot be directly converted, as the molecular weight varies between specific lipid species. Hence, average molecular weights need to be estimated in both permissive and restrictive approaches, leading to skewed predictions.

2.2. Representing lipid constraints with the aid of SLIME reactions

In this study we solve the problems presented above through two new types of pseudo-reactions, to account for both constraints on lipid classes and on acyl chains. The first pseudo-reactions **S**plit **L**ipids **I**nto **M**easurable **E**ntities and are hence referred to as SLIME reactions. As the name suggests, these pseudo-reactions take each specific lipid and split it into its basic components, i.e. its backbone and acyl chains:

$$\mathrm{L_{ij}} \rightarrow s_B\ \mathrm{B_i} + \sum_{k \in j} s_{jk}\ \mathrm{C_k} \qquad [\mathrm{Eq.}\,7]$$

where L_{ij} is a lipid of class i and chain configuration j, B_i the corresponding backbone, C_k the corresponding chain k, and s_B and s_{jk} the associated stoichiometry coefficients. These reactions replace any pseudo-reaction of the sort of Eq.5 or Eq.6 that were already present in the model (Figure 1).

The second type of pseudo-reactions are new lipid pseudo-reactions, which will in turn replace Eq.4, the old lipid pseudo-reaction that only constrained lipid classes. There are now three

different lipid pseudo reactions (Figure 1): the first pulls all backbone species created in Eq.7 into a generic backbone and uses the corresponding abundance data [g/gDW] as stoichiometric coefficients. The second reaction does the same with the specific acyl chains, with the data from FAME analysis [g/gDW], to create a generic acyl chain. Finally, the third reaction merges back together the generic backbone and the generic acyl chain into a generic lipid, which will be used in the biomass pseudo-reaction as in Eq.2.

For the new reactions to be consistent, we need to choose adequate stoichiometric coefficients for Eq.7. If the abundance data would be molar, s_B would be equal to 1 and s_{jk} would be equal to the number of repetitions of the corresponding acyl chain in the lipid. However, as the abundance data often comes in mass units, s_B must be equal to the molecular weight [g/mmol] of the full lipid, and s_{jk} must be equal to the molecular weight of the corresponding acyl chain k, multiplied by the number of repetitions of k in configuration j. By choosing these values we allow the SLIME reactions to convert the molar production of the lipid [mmol/gDWh] into a mass basis [g/gDWh], which in turn will be converted to a lipid turnover [1/h] by the lipid pseudo reactions.

2.3. Data used

All data used in this study was collected from literature. For the main model analysis (section 3.1) and the analysis of lipid metabolism under increasing levels of stress (section 3.3), aerobic glucose-limited chemostat data of *S. cerevisiae*, strain CEN.PK113-7D, growing on minimal media at a growth rate of D = 0.1 h^{-1} was used (Lahtvee *et al*, 2017). The mentioned study collected lipid abundance data in mg/gDW for both lipid classes and acyl chains for 1 reference condition plus 9 different conditions of stress (temperature, ethanol and osmotic stress). Additionally, carbohydrate, protein and RNA content [g/gDW] was measured for all stress conditions, together with flux data [mmol/gDWh] for glucose and oxygen uptake, and glycerol, acetate, ethanol, pyruvate, succinate and CO_2 production.

For model validation (section 3.2), aerobic data of *S. cerevisiae*, strain BY4741, grown on SD media at maximum growth rate (shake flask cultures) was used (Ejsing *et al*, 2009). The authors from that study introduced a novel quantification method for detecting the abundance of up to 250 singular species of lipids. Out of those, 102 were used in our study as they had direct correspondence to a species in the GEM employed. Those species represented on average 84% of

the total detected lipid abundance, which was considered high enough to proceed with the rest of the analysis. The values were converted from mol/mol to mg/gDW assuming an 8% lipid abundance in biomass (Lahtvee *et al*, 2017) and considering the unmatched lipid percentage previously mentioned. Additionally, a protein composition of 0.5 g/gDW, an RNA composition of 0.06 g/gDW, a glucose uptake of 20.4 mmol/gDWh, and biomass growth rate of 0.41 h^{-1} were assumed based on previous batch simulations of the yeast GEM (Sánchez *et al*, 2017).

2.4. Model building details

The consensus genome-scale model of yeast (version 7.8.0) was obtained from https://github.com/SysBioChalmers/yeast-GEM/releases/tag/v7.8.0. Compared to the published version (Aung *et al*, 2013), the model included several manual curations detailed in previous work (Sánchez *et al*, 2017), a clustered biomass pseudo-reaction, and metabolite formulas added to every lipid. Combining this model together with the experimental data, the following 5 steps were followed to create a model with SLIME reactions, specific to each experimental condition:

1. Add pseudo-metabolites representing each specific backbone, each specific acyl chain, the generic backbone and the generic acyl chain.
2. Add for each specific lipid species a SLIME reaction, as described in section 2.2. These reactions replace the previous ones of the sort of Eq.6 in the model (Heavner *et al*, 2012).
3. Add all three lipid pseudo-reactions described in section 2.2 using the experimental data [g/gDW]. These reactions replace the previous lipid pseudo-reaction.
4. Scale either the lipid class or the acyl chain abundancy data so that they are proportional, as the approach is based on exact mass balances. For this, an optimization problem is carried out where the coefficients of the corresponding pseudo-reaction are rescaled to minimize to zero the excretion of unused backbones and acyl chains (Figure S1).
5. Finally, scale any other component in the biomass pseudo-reaction for which there is data, and ensure that the biomass composition adds up to 1 g/gDW (Chan *et al*, 2017) by rescaling the total amount of carbohydrates, which was not measured in the datasets employed.

To compare the performance of the new enhanced model, an additional model for each condition was created, which did not have the acyl chain pseudo-reaction, but instead exchange reactions

for each acyl chain, so that the model could choose freely the acyl chain distribution. We refer to this model in the following as the "permissive" model, and use it to benchmark our analysis.

2.5. Simulation details

For all FBA simulations, measured exchange fluxes were used to constrain the model, ATP requirements were removed, and a parsimonious FBA approach (Lewis *et al*, 2010) was followed, maximizing first the ATP turnover and then minimizing the total sum of absolute fluxes, in order to find the most compact solution. The obtained objective function value was stored to compare ATP costs from transitioning from one state to another.

The variability of each different lipid species was computed in section 3.1 with flux variability analysis (FVA) (Mahadevan & Schilling, 2003) to each corresponding group of SLIME reactions at a time; e.g., for assessing the variability of C18:0 in PI, FVA was applied to all SLIME reactions producing PI and any C18:0 acyl chains. Variability was also assessed in section 3.2 with an artificial centering hit-and-run implementation of random sampling (Megchelenbrink *et al*, 2014). Abundances in mg/gDW of each lipid species were then computed from the corresponding SLIME reaction fluxes, multiplied by the molecular weight and divided by the biomass growth rate. Simulations were all performed using the COBRA toolbox for Matlab® (Becker *et al*, 2007; Schellenberger *et al*, 2011; Heirendt *et al*, 2017) with Gurobi® 7.5 set as optimizer.

3. Results

3.1. Improved model of yeast

We implemented SLIMEr in the consensus genome-scale model of yeast version 7.8.0, which had at the start 2224 metabolites and 3496 reactions. Out of those reactions, 176 corresponded to reactions of the sort of Eq.6, which were replaced by 186 SLIME reactions that cover in total 19 lipid classes and 6 different acyl chains. An additional 27 metabolites (including both specific and generic backbones and acyl chains) and 15 reactions (including transport reactions, lipid pseudo-reactions and exchange reactions) were added to the model, and 10 metabolites and 1

reaction (connected to previously deleted reactions) were removed. The final enhanced model had therefore 2241 metabolites and 3520 reactions.

In this section, we used lipid data from a study (Lahtvee *et al*, 2017) where both lipid profiling and FAME analysis were conducted. The former was rescaled to be proportional to the latter, as detailed in section 2.4. After using SLIMEr, as expected, the enhanced model predicted the same acyl chain distribution as the experimental data (Figure 2A), whereas the permissive model predicted mostly acyl chains of 16-carbon length (less costly), and only a small amount of 18-carbon length to satisfy the requirement of ergosterol ester (Figure S2), as ergosteryl oleate is cheaper to produce mass-wise than ergosteryl palmitoleate (Table S1).

With the enhanced model we also studied in how many ways lipid requirements can be satisfied spending the same amount of energy, by performing FVA (Mahadevan & Schilling, 2003) at the optimal objective function value (Figure 2B). Comparing these predictions to the ones of the permissive model (Figure S2), we saw some reductions in variability, coming mostly from changes in phosphatidylcholine and triglyceride content. However, despite the additional constraints imposed, lipid metabolism could still rearrange itself in a wide amount of combinations. This agrees with experimental observations that lipid metabolism is highly flexible (Ejsing *et al*, 2009). Therefore, handling lipid metabolism as presented here is preferred over alternative approaches, such as models that constrain single individual lipid species (Mardinoglu *et al*, 2014; Monk *et al*, 2017), as these limit the organism to only one feasible state of lipid metabolism and hence bias results.

3.2. Model predictions versus experimental data

To validate model predictions, we used data from literature (Ejsing *et al*, 2009) where each specific lipid species was measured (section 2.3). This data was added up to compute the totals of each lipid class and each acyl chain, and these sums were in turn used as input for creating both a permissive and an enhanced model. In this case, as a total lipid abundance of 8% was assumed, the acyl chains abundances were rescaled to be proportional to the lipid classes abundances (section 2.4).

We then performed random sampling (Megchelenbrink *et al*, 2014) on the resulting models, to generate 10,000 flux distributions for each model and for each of the 8 conditions of the study (4 different strains cultivated at 2 different temperatures). The simulation results of the enhanced

model for the reference condition are shown in Figure 3A. Comparing the *in silico* lipid compositions to the original *in vivo* measurements, the enhanced model improved the average prediction error for all experimental conditions (Table S2), and overall the simulated lipid distributions came much closer to the experimental values compared to the permissive model (Figure 3B).

It should be noted that even though SLIMEr improved the model's lipid composition predictions, many other distributions were still predicted to be equally likely, both for the reference condition (Figure 3A) and all 4 strains (Figure 3B, Figure S3). This highlights the high level of regulation in place to adapt the distribution of lipid species in *S. cerevisiae* depending on the environmental conditions.

3.3. Energy costs at increasing levels of stress

By using SLIMEr, we can better represent the lipid expenses of transitioning from a metabolic state of low energy demand to high energy demand. To show this we integrated data of yeast grown under different levels of stress (Lahtvee *et al*, 2017), as these stress levels were previously correlated to an increase in maintenance energy (Lahtvee *et al*, 2016). Comparing simulations for the reference condition (same as in section 3.1), the permissive model could produce 101.7 µmol(ATP)/gDW more than the enhanced model, which corresponds to the extra energy required to achieve the acyl chain distribution. By repeating the analysis for all 9 conditions of stress, we found that both the extra energy and carbon expenses increased as the stress levels increased (Figure 3C), which was associated to an increase in maintenance energy (Figure S4).

In the reference condition, the simulated growth-associated maintenance requirement (GAM) without accounting for known polymerization costs of proteins, carbohydrates, RNA and DNA (Förster *et al*, 2003) was 35.14 mmol(ATP)/gDW, which corresponds to the maintenance costs of unspecified functions in the model, such as protein turnover, maintenance of membrane potentials, etc. The ATP cost for achieving correct acyl chain distribution under reference conditions corresponded then to 0.3% of the total costs of processes not include in the model.

4. Discussion

With SLIMEr we can now correctly represent the biomass requirements from lipid metabolism in genome-scale metabolic models. The approach allows the model to satisfy at the same time requirements on the lipid class and acyl chain distributions, which is a significant improvement compared to only being able to constrain lipid classes (Aung *et al*, 2013; Brunk *et al*, 2018). We have also shown the high degree of flexibility in lipid metabolism, which shows that approaches that over-constrain the lipid requirements by enforcing specific concentrations for individual species (Mardinoglu *et al*, 2014; Monk *et al*, 2017; Lachance *et al*, 2018) or forcing a given acyl chain distribution to all species (Nookaew *et al*, 2008; Kerkhoven *et al*, 2016) are not suitable for handling this flexibility. Finally, we have demonstrated the use of the expanded model as a tool to compute lipid requirements in varying experimental conditions.

It is important to note that the model does not take other physiological properties into account, such as curvature and fluidity of membranes as function of lipid composition and/or temperature, as well as specific regulation. It only takes FAME analysis and lipid profile, and demonstrates that specific lipid distributions are consistent with these measurements. It would be of interest to also account for additional data and processes such as the ones mentioned, but this is beyond the scope of this study.

Even though developed for *S. cerevisiae*, this approach can be extended to any other organism. The main challenge here is to map all lipids in the model to the corresponding pseudo-metabolites (backbones and chains), as conventions for naming lipids vary a great deal between different databases and models. Introduction of standardized metabolite ids (Brooksbank *et al*, 2005; Dräger & Palsson, 2014) can significantly aid this otherwise laborious task.

SLIMEr, together with all scripts necessary to reproduce the results presented in this study, are available at https://github.com/SysBioChalmers/SLIMEr. All new SLIME reactions and lipid pseudo-reactions have been added to the consensus GEM of yeast and are available in version 8.1.0: https://github.com/SysBioChalmers/yeast-GEM/releases/tag/v8.1.0.

Acknowledgments

The authors would like to thank Dr. Hongzhong Lu for help in annotation of lipid formulas, Dr. Petri-Jaan Lahtvee and Dr. Paulo Teixeira for aiding in data analysis, and Sebastián Mendoza for suggesting the random sampling approach. This project has received funding from the European Union's Horizon 2020 research and innovation program under grant agreement No 686070, Knut and Alice Wallenberg Foundation and the Novo Nordisk Foundation. BJS acknowledges financial support from CONICYT (grant #6222/2014), and EJK acknowledges financial support from Åforsk Foundation.

Author contributions

JN and BJS conceived the project. BJS, FL and EJK designed the mathematical formulation. BJS implemented the algorithm and performed all computational simulations. BJS and FL processed the literature data. BJS wrote the original draft. All authors read, edited and approved the final manuscript.

References

Abdulkadir S & Tsuchiya M (2008) One-step method for quantitative and qualitative analysis of fatty acids in marine animal samples. *J. Exp. Mar. Bio. Ecol.* **354:** 1–8

Aung HW, Henry SA & Walker LP (2013) Revising the Representation of Fatty Acid, Glycerolipid, and Glycerophospholipid Metabolism in the Consensus Model of Yeast Metabolism. *Ind. Biotechnol.* **9:** 215–228

Becker SA, Feist AM, Mo ML, Hannum G, Palsson BØ & Herrgård MJ (2007) Quantitative prediction of cellular metabolism with constraint-based models: the COBRA Toolbox. *Nat. Protoc.* **2:** 727–738

Brooksbank C, Cameron G & Thornton J (2005) The European Bioinformatics Institute's data resources: Towards systems biology. *Nucleic Acids Res.* **33:** 46–53

Brunk E, Sahoo S, Zielinski DC, Altunkaya A, Dräger A, Mih N, Gatto F, Nilsson A, Preciat Gonzalez GA, Aurich MK, Prlić A, Sastry A, Danielsdottir AD, Heinken A, Noronha A, Rose PW, Burley SK, Fleming RMT, Nielsen J, Thiele I, et al (2018) Recon3D enables a three-dimensional view of gene variation in human metabolism. *Nat. Biotechnol.* **36:** 272–281

Chan SHJ, Cai J, Wang L, Simons-Senftle MN & Maranas CD (2017) Standardizing biomass

reactions and ensuring complete mass balance in genome-scale metabolic models. *Bioinformatics* **33:** 3603–3609

Dikicioglu D, Kırdar B & Oliver SG (2015) Biomass composition: the 'elephant in the room' of metabolic modelling. *Metabolomics* **11:** 1690–1701

Dobson PD, Smallbone K, Jameson D, Simeonidis E, Lanthaler K, Pir P, Lu C, Swainston N, Dunn WB, Fisher P, Hull D, Brown M, Oshota O, Stanford NJ, Kell DB, King RD, Oliver SG, Stevens RD & Mendes P (2010) Further developments towards a genome-scale metabolic model of yeast. *BMC Syst. Biol.* **4:** 145

Dräger A & Palsson BØ (2014) Improving collaboration by standardization efforts in systems biology. *Front. Bioeng. Biotechnol.* **2:** 1–20

Ejsing CS, Sampaio JL, Surendranath V, Duchoslav E, Ekroos K, Klemm RW, Simons K & Shevchenko A (2009) Global analysis of the yeast lipidome by quantitative shotgun mass spectrometry. *Proc. Natl. Acad. Sci.* **106:** 2136–2141

Feist AM & Palsson BO (2010) The biomass objective function. *Curr. Opin. Microbiol.* **13:** 344–349

Förster J, Famili I, Palsson BØ & Nielsen J (2003) Genome-Scale Reconstruction of the Saccharomyces Cerevisie Metabolic Network. *Genome Res.* **13:** 244–253

Heavner BD, Smallbone K, Barker B, Mendes P & Walker LP (2012) Yeast 5 - an Expanded Reconstruction of the Saccharomyces Cerevisiae Metabolic Network. *BMC Syst. Biol.* **6:** 1

Heavner BD, Smallbone K, Price ND & Walker LP (2013) Version 6 of the consensus yeast metabolic network refines biochemical coverage and improves model performance. *Database* **2013:** bat059

Heirendt L, Arreckx S, Pfau T, Mendoza SN, Richelle A, Heinken A, Haraldsdóttir HS, Wachowiak J, Keating SM, Vlasov V, Magnusdóttir S, Ng CY, Preciat G, Žagare A, Chan SHJ, Aurich MK, Clancy CM, Modamio J, Sauls JT, Noronha A, et al (2017) Creation and analysis of biochemical constraint-based models: the COBRA Toolbox v3.0. Available at: http://arxiv.org/abs/1710.04038 [Accessed May 15, 2018]

Herrgård MJ, Swainston N, Dobson PD, Dunn WB, Arga KY, Arvas M, Blüthgen N, Borger S, Costenoble R, Heinemann M, Hucka M, Le Novère N, Li P, Liebermeister W, Mo ML, Oliveira AP, Petranovic D, Pettifer S, Simeonidis E, Smallbone K, et al (2008) A consensus yeast metabolic network reconstruction obtained from a community approach to systems biology. *Nat. Biotechnol.* **26:** 1155–60

Kerkhoven EJ, Pomraning KR, Baker SE & Nielsen J (2016) Regulation of amino-acid metabolism controls flux to lipid accumulation in Yarrowia lipolytica. *npj Syst. Biol. Appl.* **2:** 16005

Khoomrung S, Chumnanpuen P, Jansa-Ard S, Ståhlman M, Nookaew I, Borén J & Nielsen J (2013) Rapid Quantification of Yeast Lipid using Microwave-Assisted Total Lipid Extraction and HPLC-CAD. *Anal. Chem.* **85:** 4912–4919

Lachance J-C, Monk JM, Lloyd CJ, Seif Y, Palsson BO, Rodrigue S, Feist AM, King ZA & Jacques P-E (2018) BOFdat: generating biomass objective function stoichiometric coefficients from experimental data. *bioRxiv***:** 243881

Lahtvee P-J, Kumar R, Hallström B & Nielsen J (2016) Adaptation to different types of stress converge on mitochondrial metabolism. *Mol. Biol. Cell* **27:** 2505–2514

Lahtvee PJ, Sánchez BJ, Smialowska A, Kasvandik S, Elsemman IE, Gatto F & Nielsen J (2017) Absolute Quantification of Protein and mRNA Abundances Demonstrate Variability in Gene-Specific Translation Efficiency in Yeast. *Cell Syst.* **4:** 495–504

Lewis NE, Hixson KK, Conrad TM, Lerman JA, Charusanti P, Polpitiya AD, Adkins JN, Schramm G, Purvine SO, Lopez-Ferrer D, Weitz KK, Eils R, König R, Smith RD & Palsson BØ (2010) Omic data from evolved E. coli are consistent with computed optimal growth from genome-scale models. *Mol. Syst. Biol.* **6:** 390

Mahadevan R & Schilling CH (2003) The effects of alternate optimal solutions in constraint-based genome-scale metabolic models. *Metab. Eng.* **5:** 264–276

Mardinoglu A, Agren R, Kampf C, Asplund A, Uhlen M & Nielsen J (2014) Genome-scale metabolic modelling of hepatocytes reveals serine deficiency in patients with non-alcoholic fatty liver disease. *Nat. Commun.* **5:** 3083

Megchelenbrink W, Huynen M & Marchiori E (2014) optGpSampler: An improved tool for uniformly sampling the solution-space of genome-scale metabolic networks. *PLoS One* **9:** e86587

Monk JM, Lloyd CJ, Brunk E, Mih N, Sastry A, King Z, Takeuchi R, Nomura W, Zhang Z, Mori H, Feist AM & Palsson BO (2017) iML1515, a knowledgebase that computes Escherichia coli traits. *Nat. Biotechnol.* **35:** 904–908

Nielsen J (2017) Systems Biology of Metabolism. *Annu. Rev. Biochem.* **86:** 245–275

Nookaew I, Jewett MC, Meechai A, Thammarongtham C, Laoteng K, Cheevadhanarak S, Nielsen J & Bhumiratana S (2008) The genome-scale metabolic model iIN800 of Saccharomyces cerevisiae and its validation: a scaffold to query lipid metabolism. *BMC Syst. Biol.* **2:** 71

Orth JD, Thiele I & Palsson BØ (2010) What is flux balance analysis? *Nat. Biotechnol.* **28:** 245–248

Sánchez BJ, Zhang C, Nilsson A, Lahtvee P, Kerkhoven EJ & Nielsen J (2017) Improving the phenotype predictions of a yeast genome□scale metabolic model by incorporating enzymatic constraints. *Mol. Syst. Biol.* **13:** 935

Schellenberger J, Que R, Fleming RMT, Thiele I, Orth JD, Feist AM, Zielinski DC, Bordbar A, Lewis NE, Rahmanian S, Kang J, Hyduke DR & Palsson BØ (2011) Quantitative prediction of cellular metabolism with constraint-based models: the COBRA Toolbox v2.0. *Nat. Protoc.* **6:** 1290–1307

Figure Index

Figure 1: Overview of the process of including SLIME reactions and new lipid pseudo-reactions for a hypothetical model of 3 lipid classes (yellow, orange and red) and 2 types of acyl-chain (blue and red). Generic backbones/acyl chains are in turn colored black. The active fluxes after a simulation are highlighted in light blue before and after using the method, showing that a GEM with a restrictive approach would use the same acyl chain composition for all lipid classes (left upper corner), a GEM with a permissive approach would always choose the cheapest species from each lipid class (left lower corner), and a GEM with SLIME reactions would satisfy both the lipid class and the acyl chain distribution, but choosing freely which specific lipid species to produce for this goal (right side).

Figure 2: The enhanced GEM with improved constraints on lipid metabolism. **(A)** By using SLIMEr, a correct acyl chain composition is achieved. **(B)** Breakdown of the acyl chain distribution and variability predicted by the enhanced GEM, for each experimentally detected lipid class. Dark lines correspond to parsimonious FBA predictions, while the FVA allowed ranges are shown with colored bars. PI: phosphatidylinositol. SE: ergosterol ester. FFA: free fatty acid. PS: phosphatidylserine. PC: phosphatidylcholine. PE: phosphatidylethanolamine. TAG: triglyceride.

Figure 3: Using experimental data to validate the model and predict energy costs. **(A)** The lipid composition of 10,000 simulations of the enhanced model achieved with random sampling are presented for each specific lipid species (blue circles), compared to the actual measured experimental values (red bars). TAG: triglyceride. DAG: diglyceride. PA: phosphatidate. PS: phosphatidylserine. PE: phosphatidylethanolamine. PC: phosphatidylcholine. LPI: lysophosphatidylinositol. PI: phosphatidylinositol. PG: phosphatidylglycerol. CL: cardiolipin. LCB: long-chain base. LCBP: long-chain base phosphate. Cer: ceramide. IPC: inositolphosphoceramide. MIPC: mannosyl-inositolphosphoceramide. M(IP)2C: mannosyl-diinositolphosphoceramide. **(B)** Principal component analysis (PCA) of all (log transformed) lipid abundance distributions for both the permissive model (yellow) and the enhanced model (blue), compared to experimental values (red, in bold). Different tonalities of yellow and blue

indicate the 2 different simulated conditions for the 4 different strains. **(C)** Costs in terms of both carbon (continuous lines) and ATP (segmented lines) of satisfying the acyl chain distribution at 3 increasing levels of stress of temperature (33, 36 and 38ºC; red), NaCl concentrations (200, 400 and 600 mM; blue) and EtOH concentrations (20, 40 and 60 g/L; green).

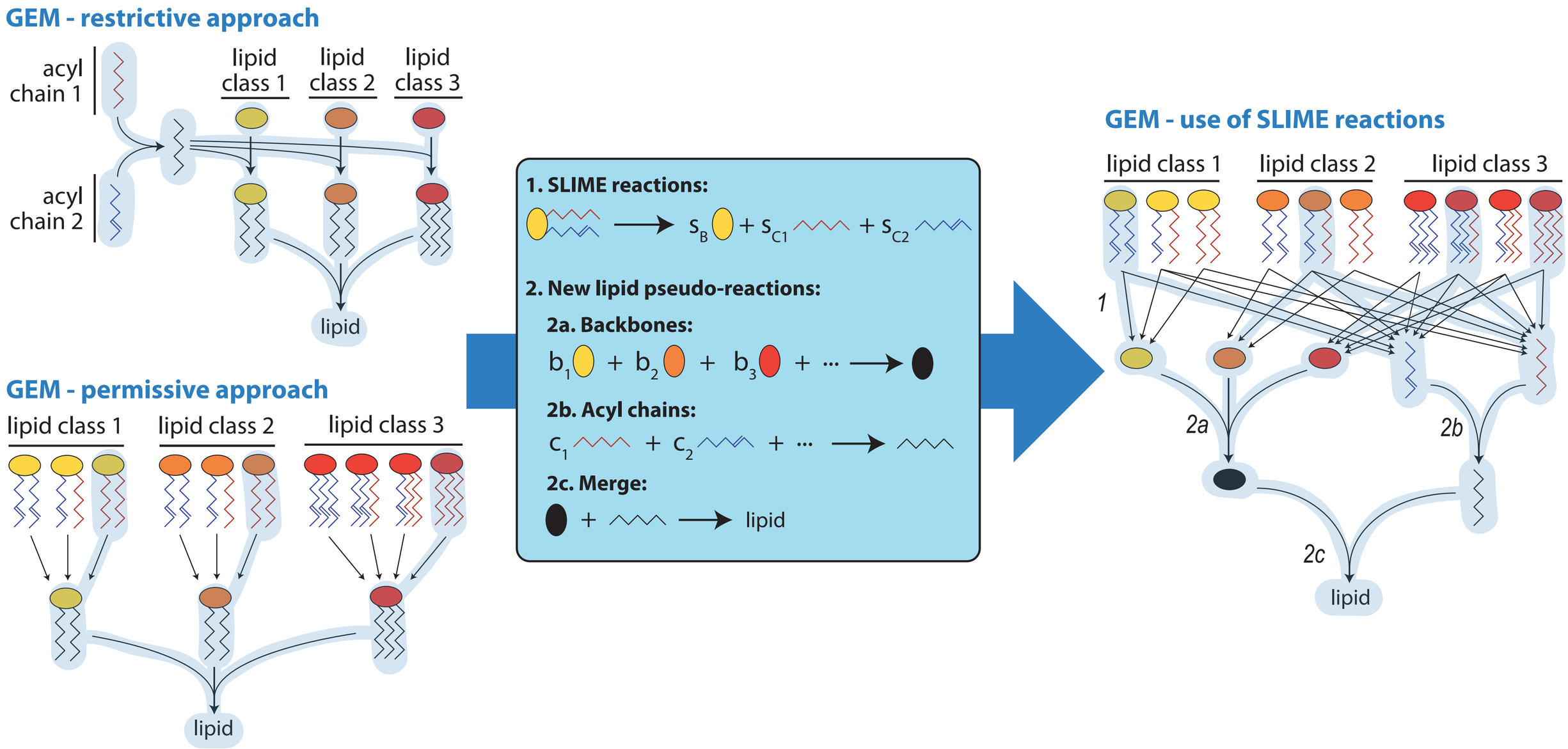
GEM - restrictive approach
acyl chain 1
acyl chain 2
lipid class 1
lipid class 2
lipid class 3
lipid
GEM - permissive approach
lipid class 1
lipid class 2
lipid class 3
lipid
1. SLIME reactions:
s_B + s_{C1} + s_{C2}
2. New lipid pseudo-reactions:
2a. Backbones:
b_1 + b_2 + b_3 + ...
2b. Acyl chains:
c_1 + c_2 + ...
2c. Merge:
+ lipid
GEM - use of SLIME reactions
lipid class 1
lipid class 2
lipid class 3
1
2a
2b
2c
lipid

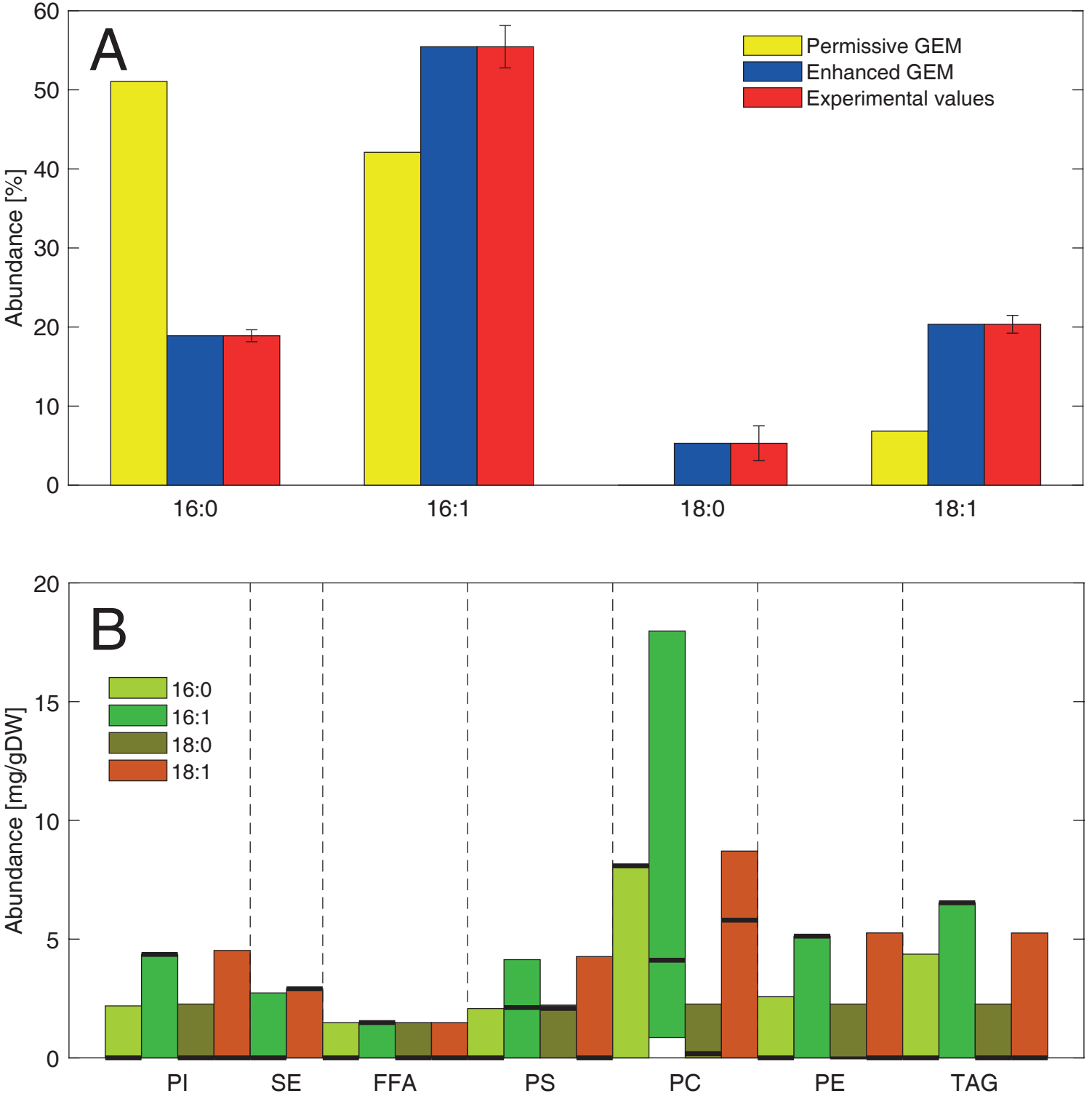
A
Permissive GEM
Enhanced GEM
Experimental values
Abundance [%]
0
10
20
30
40
50
60
16:0
16:1
18:0
18:1
B
16:0
16:1
18:0
18:1
Abundance [mg/gDW]
0
5
10
15
20
PI
SE
FFA
PS
PC
PE
TAG

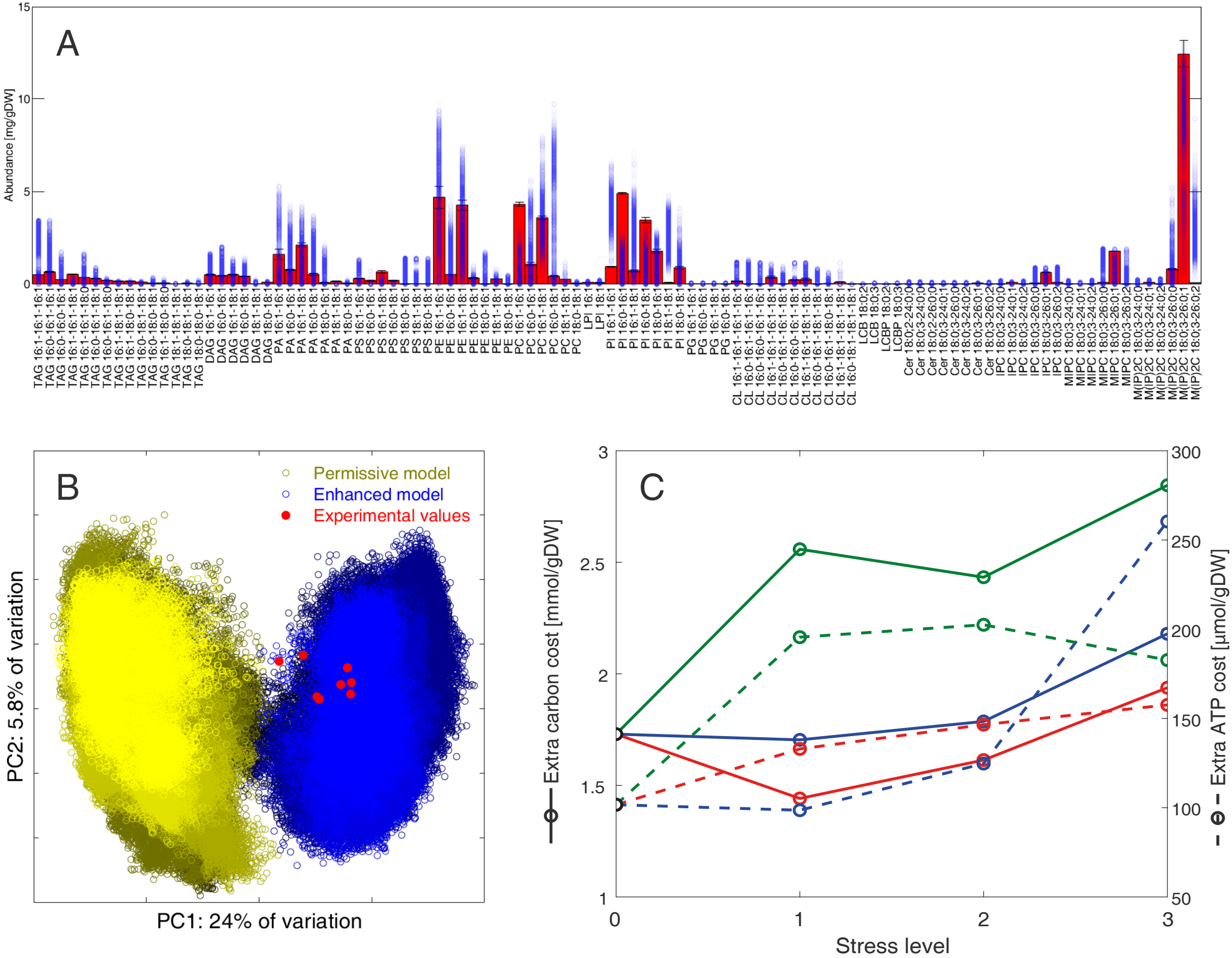
A
Abundance [mg/gDW]
B
Permissive model
Enhanced model
Experimental values
PC2: 5.8% of variation
PC1: 24% of variation
C
Extra carbon cost [mmol/gDW]
Extra ATP cost [µmol/gDW]
Stress level